



Radiological Investigation of Gas Embolism in the East Asian Finless Porpoise (*Neophocaena asiaeorientalis sunameri*)

Adams Hei Long Yuen^{1,2†}, Sang Wha Kim^{1†}, Sung Bin Lee¹, Seyoung Lee³, Young Ran Lee^{1,4}, Sun Min Kim⁵, Cherry Tsz Ching Poon⁶, Jun Kwon¹, Won Joon Jung¹, Sib Sankar Giri¹, Sang Guen Kim¹, Jeong Woo Kang¹, Young Min Lee¹, Jong-pil Seo³, Byung Yeop Kim^{7*} and Se Chang Park^{1*}

¹ College of Veterinary Medicine and Research Institute for Veterinary Science, Seoul National University, Seoul, South Korea, ² Department of Radiotherapy, Hong Kong Sanatorium and Hospital, Happy Valley, Hong Kong SAR, China, ³ College of Veterinary Medicine and Veterinary Medical Research Institute, Jeju National University, Jeju, South Korea, ⁴ Conservation Department, World Wide Fund for Nature - Korea, Seoul, South Korea, ⁵ Department of Parasitology and Parasite Research Center, College of Medicine, Chungbuk National University, Cheongju, South Korea, ⁶ Department of Surgery, Queen Mary Hospital, Pokfulam, Hong Kong SAR, China, ⁷ Department of Marine Industrial and Maritime Police, College of Ocean Science, Jeju National University, Jeju, South Korea

OPEN ACCESS

Edited by:

Satya Panigrahi,
Indira Gandhi Centre for Atomic
Research (IGCAR), India

Reviewed by:

Sadayan Paramasivam,
Alagappa University, India
Hui Yang,
Yangzhou University, China

*Correspondence:

Byung Yeop Kim
kimby@jejunu.ac.kr
Se Chang Park
parksec@snu.ac.kr

†These authors have contributed
equally to this work

Specialty section:

This article was submitted to
Marine Biology,
a section of the journal
Frontiers in Marine Science

Received: 18 May 2021

Accepted: 18 February 2022

Published: 24 March 2022

Citation:

Yuen AHL, Kim SW, Lee SB,
Lee S, Lee YR, Kim SM, Poon CTC,
Kwon J, Jung WJ, Giri SS, Kim SG,
Kang JW, Lee YM, Seo J-p, Kim BY
and Park SC (2022) Radiological
Investigation of Gas Embolism
in the East Asian Finless Porpoise
(*Neophocaena asiaeorientalis*
sunameri). *Front. Mar. Sci.* 9:711174.
doi: 10.3389/fmars.2022.711174

Cetaceans have long been considered biologically adapted to suffer no adverse effects from diving-related tissue gas tension. However, increasing reports of gas embolism in cetaceans inhabiting European, Mediterranean and American waters have challenged the conventional understanding of marine mammal diving physiology. In human hyperbaric medicine, virtopsy techniques such as post-mortem computed tomography (PMCT) facilitate the visualization of gas embolism and could be performed adjunct to conventional autopsy. This research presents the first case of gas embolism identified in an East Asian finless porpoise inhabiting Asian waters. Massive gas embolic lesions were found in the liver, which had been compressing both the lungs and abdominal organs, and signs of pneumonia and parasitic infection were observed in both lungs. It is hypothesized that this porpoise might have been unable to expel *in vivo* gas bubbles from its circulation due to pulmonary dysfunction. Consequently, gas bubbles agglomerated in the liver, resulting in the development of gas embolic lesions. The findings of the present study provide insights into the occurrence of gas embolism in the East Asian finless porpoise, highlighting the potential of PMCT as a promising tool for the diagnosis of gas embolism in stranded cetaceans.

Keywords: cetaceans, post-mortem computed tomography, virtopsy, gas embolism, tissue gas tension, hyperbaric, East Asian finless porpoise

INTRODUCTION

There has been longstanding debate over the effects of tissue gas tension in marine mammals (Kooyman et al., 1972; Ridgway and Howard, 1979). Previous studies have suggested that cetaceans can prevent the formation of gas emboli through behavioral, physiological, and anatomical adaptations (Blix et al., 2013; Elmegaard et al., 2016; Fahlman et al., 2021). However, evidence of gas embolism occurring in cetaceans has challenged the conventional understanding of marine

mammal diving physiology (Southall et al., 2016). The development of abnormal gas bubble lesions in these animals has been gaining interest among marine mammal scientists since the publication of the work by Jepson et al. (2003). Gas embolism has been recorded mainly in beaked whales (family *Ziphiidae*), and sporadically in certain dolphin species (Moore et al., 2009; Dennison et al., 2012; Fernández et al., 2017; Denk et al., 2020). It is believed that cetaceans may develop gas embolism due to dramatic reactions to anthropogenic activities (Jepson et al., 2003; Moore et al., 2009) or alterations in diving behavior (Fernández et al., 2017).

In human hyperbaric medicine, computed tomography (CT) is one of the most commonly used techniques used to detect gas embolism (Laurent et al., 2014; Schwartz et al., 2018). Moreover, post-mortem computed tomography (PMCT) has become more accessible as an adjunct to conventional autopsies, in forensic settings. PMCT facilitates visualization of gas embolism (Plattner et al., 2003; Chou et al., 2016) and detection of abnormal gas space volume, which are often difficult to detect in conventional autopsies (Plattner et al., 2003). As CT has become more readily available in veterinary research facilities, PMCT has also been used to investigate the cause of death, pathological and biological profile in cetaceans (Yuen et al., 2016, 2017; Cuvertoret-Sanz et al., 2020; Kot et al., 2020).

East Asian finless porpoises (*Neophocaena asiaorientalis sunameri*) are frequently found in the coastal waters of Northeast Asia (Jefferson and Hung, 2004), where increasing anthropogenic activities pose a potential threat to the porpoise population (Xiong et al., 2018; Cheng et al., 2021), such as peracute underwater entrapment. The cause of death of East Asian finless porpoises stranded in South Korean waters has recently been assessed by PMCT to provide information complementary to conventional necropsy findings. In this manuscript, we describe the radiological appearance, together with necropsy and histological findings of gas embolism in an East Asian finless porpoise, stranded on Jeju Island in the Republic of Korea; this study represents the first identified occurrence of gas embolism in this species.

MATERIALS AND METHODS

Cetacean Carcass Obtained for Investigation

In November 2020, an adult male East Asian finless porpoise, measuring 127.6 cm in length, was stranded on the northern coast of Jeju Island in the Republic of Korea (33°33.480'N 126°44.686'E). The average ambient temperature and seawater temperature of the location was 8.6 and 17.6°C, respectively. No scavengers were found upon carcass retrieval. The carcass was classified as code 2—fresh carcass—according to the Smithsonian condition codes (Geraci and Lounsbury, 2005). Post-mortem staining was not observed on the carcass body. To minimize post-mortem changes, the carcass was directly transported to the freezer in the Jeju National University within 2 h after it was first reported to the marine police and frozen at -22°C until further examinations could be conducted. Ethical review and approval

were not required, since no aspect of the animal's life was altered for the present study.

Performance of Virtopsy

The carcass was transported to the Jeju National University Equine Hospital for PMCT scanning, which is located at a 5-min distance by vehicle. PMCT scanning was done using an Aquilion Lightning 16-row, 32-slice helical CT system (Aquilion Lightning, Canon Medical Systems, Otawara, Japan). The X-ray tube of the CT scanner was warmed up prior to taking the carcass from the freezer in order to prevent the carcass from thawing. The scan was performed at 120 kVp, 200 mAs, and 2 mm slice thickness, while the scan field of view (sFOV) was set to 320 mm. To minimize post-mortem changes, the whole procedures were limited to less than 30 min. The average ambient temperature on the day was 10°C, the whole virtopsy procedures were finished before the body started to thaw. CT images were then assessed using open-source Digital Imaging and Communications in Medicine (DICOM) viewing software, Horos version 3.3.6 (RRID:SCR_017340).¹

Performance of Necropsy and Histology

The carcass was thawed for 36 h in ambient temperature (average 11.05°C) prior to necropsy. The carcass condition was closely monitored by board-certified veterinarians to avoid excessive decomposition. All the board-certified veterinarians who participated in the necropsy agreed that the carcass was in a fresh state upon necropsy based on the observation of the external body feature and the conditions of the internal organs. Standard necropsy protocol was followed for the marine mammals (Pugliarès et al., 2007). Tissue samples from the liver, kidneys, stomach, mesenteric lymph node, and lungs were collected for histological studies, which organs were selected based on the *in vivo* bubble appearance frequency by organs (Jepson et al., 2005). All samples were fixed with 10% neutral-buffered formalin (NBF) (Duksan General Science, Seoul, South Korea) at a 10:1 fixative-to-tissue ratio, before being processed into paraffin wax, and sectioned. The tissue slides were then stained with hematoxylin and eosin (H&E) and Masson's trichrome (MT) stains (Genoss Co., Ltd., Seoul, South Korea). Parasites were collected and stored in 70% ethanol and neutral-buffered formalin, for identification.

RESULTS

General Findings

The carcass examined in this study was emaciated, presenting with post-cranial dip—"peanut head"—and wasting of the epaxial muscle (**Figure 1A**). Girth measurements—56.9 cm at umbilical and 34.1 cm at anal level, respectively—were below normal, reflecting the wasted body condition. During the necropsy, little stomach and intestinal contents were found indicating the animal was not actively foraging. Based on PMCT images, blubber thickness in the head, axillary, mid-thoracic, umbilical, genital

¹www.horosproject.org

slit, and anal regions was lower than previously reported averages for East Asian finless porpoises (Zeng et al., 2015), further evidencing the animal's state of malnutrition (Figures 1B–G). This conclusion was confirmed during necropsy.

Findings From Liver Assessment

PMCT revealed severe liver enlargement. Massive gas embolic lesions ranging from 0.2 to 30.0 mm in diameter were observed using the lung window setting (WL/WW: –500/1,400 HU). The gas-filled cavities were encapsulated, with wall thickness ranging from 1.0 to 3.0 mm (Figure 2A). The liver parenchyma was replaced with bubble-like spherical cavities of various sizes, with diameters ranging from 0.5 to 25.0 mm, resulting in an increase in organ size (Figure 2B). The enlarged organ had been physically compressing the abdominal organs posteriorly and the lungs anteriorly, presumably resulting in decreased functioning of the compressed organs (Figure 2C). The tactile of the liver was abnormally firm that the organ was maintaining its original shape even after it was separated and taken out of the abdominal cavity. It was confirmed histologically that the majority of hepatic tissue had been replaced with gas-filled cavities that are surrounded by fibrous connective tissue. Pericavitary fibrosis was clearly identified when stained by MT stain, revealing a pattern similar to that presented in previous reports (Figures 2D–F; Jepson et al., 2005). Blood vessels and sinusoids were filled with *in vivo* bubbles (0.3–1.0 μm in diameter) that coalesced into larger cavities in some areas, which encroached the surrounding tissues (Figure 2D). These findings suggested that normal blood flow had been virtually impossible, whereas the overall distribution of bubbles in tissues and blood vessels led to the conclusion that the liver was non-functional.

Findings From Lung Assessment

Both lungs were smaller than normal—the left and right lungs measured 25.0 × 7.5 × 3.0 cm and 23.5 × 7.0 × 2.8 cm, respectively—presumably due to compression force exerted by the grossly enlarged liver. PMCT investigation using the lung window setting (WL/WW: –500/1,400 HU) revealed widespread ground-glass opacity in both lungs (Figure 3A). Small hyper-attenuated nodules in the alveoli, observed using the bone window setting (WL/WW: 300/1,500 HU) (Figure 3B), suggested the presence of fibrotic tissue. Furthermore, small gas bubbles were observed throughout the lungs (Figure 3C). Numerous nodules were found through gross pathological observation (Figure 3E). Parasites were found in the nodules, and also from the bronchioles, bronchi, and lung parenchyma (Figure 3F); the parasites were identified as *Halocercus sunameri* (Nematoda: Pseudaliidae) based on further morphological analyses (Yamaguti, 1951). Histological analysis confirmed pulmonary alveolar fibrosis in the nodular areas, supporting the PMCT findings. Small gas bubbles (<60 μm in diameter) were also recognizable on histopathology slides (Figure 3D). No foamy discharge was found in the trachea, bronchus, or bronchiole.

Findings From Kidney Assessment

The presence of gas bubbles—0.5–2.0 mm in diameter—was further observed in both kidneys during PMCT investigation,

using the bone window setting (WL/WW: 300/1,500 HU) (Figure 4A). Visual identification of gas-filled cavities between or within the reniculi proved problematic during necropsy as the lobules could be naturally separated from one another. Moreover, the renal calyces could be physically separated from the surrounding tissue by applying cutting pressure. However, numerous gas emboli of various sizes (5–350 μm) could be identified by investigating the histopathology slides of the kidney tissue (Figures 4B,C).

Other Findings

Gas bubbles ranging from 0.7 to 3.0 mm in diameter were also found from brain tissue (Figures 5A,B) (WL/WW: 152/524 HU), spinal cord (Figure 5C) (WL/WW: 152/524 HU), epaxial and cervical muscles (Figures 5C,D), and subdermal tissue (Figure 5D) (WL/WW: –500/1,400 HU) using PMCT. However, gas bubbles were too small to be visible during necropsy. Therefore, they were not able to locate for histopathological investigation.

Histological Confirmation of *in vivo* Gas Bubbles

No visible gas emboli were found in blood vessels either on the surface of various organs or in the mesenteric artery and vein, during PMCT investigation and necropsy. However, *in vivo* bubbles of less than 20 μm in diameter were identified histologically, not only in the liver, kidneys, and lungs but also in the mesenteric lymph nodes and stomach wall.

DISCUSSION

Gas embolism and development of gas embolic lesions in cetaceans have been predominantly described in beaked whales (Jepson et al., 2003; Fernández et al., 2005), and occasionally in certain dolphin species (Moore et al., 2009; Dennison et al., 2012; Fernández et al., 2017; Cuvertoret-Sanz et al., 2020; Denk et al., 2020). Extensive reported gas embolism cases have shown distinctive large cavitory lesions with pericavitary fibrosis in gross pathology and histopathology (Jepson et al., 2003, 2005; de Quirós et al., 2011; Siebert et al., 2013). The present subject has demonstrated similar pathology status as previously described: gas embolic lesions, encapsulated by fibrous tissue, had extensively replaced the liver parenchyma, resulting in loss of organ function.

There are a few mechanisms that can induce gas bubbles to an animal's organ parenchyma (Jepson et al., 2005; de Quirós et al., 2011; Danil et al., 2014). Most commonly, gas bubbles can be formed in severely decomposed carcasses as a result of postmortem changes due to bacterial reductive catalysis (Shedge et al., 2021). In the circumstance without death time estimation, it is commonly believed that gas bubbles may have been generated in this way. Bacterial reductive catalysis mechanism generally causes the liver to become spongier and more Swiss cheese-like (Shedge et al., 2021), and eventually the liver will lose its concrete shape. Another possible mechanism is a septicemia by gas producing bacteria with live animal, which could derive

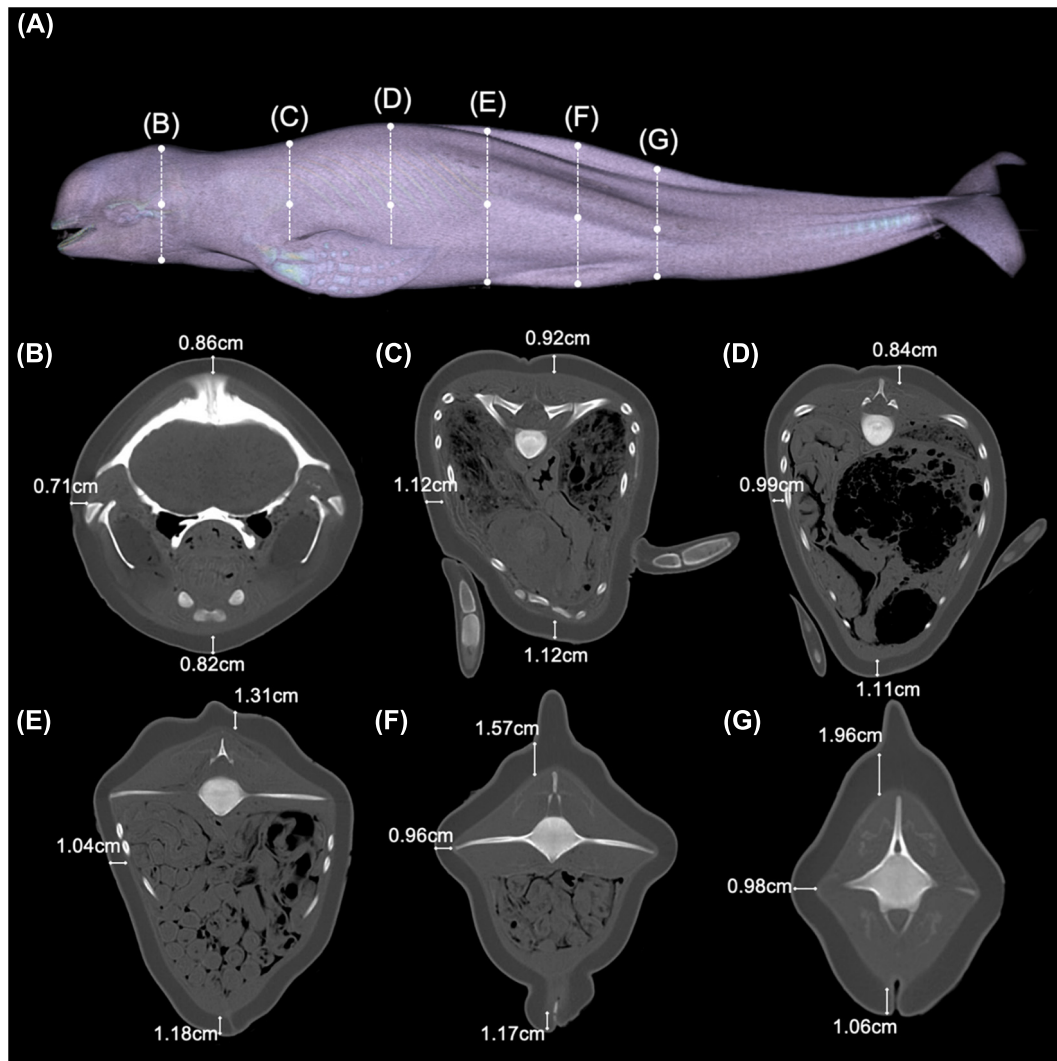


FIGURE 1 | Overview of the physical condition of an East Asian finless porpoise (*Neophocaena asiaeorientalis sunameri*) carcass. **(A)** PMCT three-dimensional surface rendered image showing the general external appearance of the East Asian finless porpoise in the present study. Dotted lines correspond to transverse CT images at **(B)** cranial, **(C)** axillary, **(D)** mid-thoracic, **(E)** umbilical, **(F)** genital slit, and **(G)** anal levels.

systemic gas bubble accumulation and eventual death (Danil et al., 2014). However, based on the previous studies, there are recognizable differences between bacterial-caused cavitation and decompression sickness-caused cavitation in both gross- and histopathological features (Jepson et al., 2003, 2005): (1) The distribution of the gas bubbles in organs is inconsistent between bacterial cavitation and decompression sickness-derived cavitation; (2) most importantly, pericavitary fibrosis is not found in the bacteria-caused gas bubble accumulations (Jepson et al., 2003, 2005). In the present study, the liver parenchyma of the East Asian finless porpoise has maintained certain shape, while the tactile is rather firm than normal (**Figure 2B**). This is due to the fibrosis progressed around the cavitory lesions as histopathology revealed (**Figure 2F**), showing a different feature from decomposed liver. Therefore, the large cavitory lesions in the liver caused by post-mortem changes or septicemia

can be ruled out. Another possible cause of the *in vivo* bubbles is frozen artifact, which still cannot explain the large-sized cavitory lesions with severely progressed fibrosis. Though post-mortem change and freeze-thaw procedure could induce histopathological artifacts, the characteristic pathologic lesions found in the liver of the current study case was obviously not one of them. Such characteristic features were possible to be seen in gas embolism cases in cetaceans, which led to the diagnosis of the current study case.

The pathogenesis of gas embolic lesions in cetaceans was recently intimated by Fahlman et al. (2021), stating that the amount of gas—particularly nitrogen—dissolved in bodily tissues is positively associated with the level and duration of a change in pressure. Exposure to elevated ambient pressure during diving causes an accumulation of dissolvable gas in tissues until a state of equilibrium with the environment, i.e., saturation has

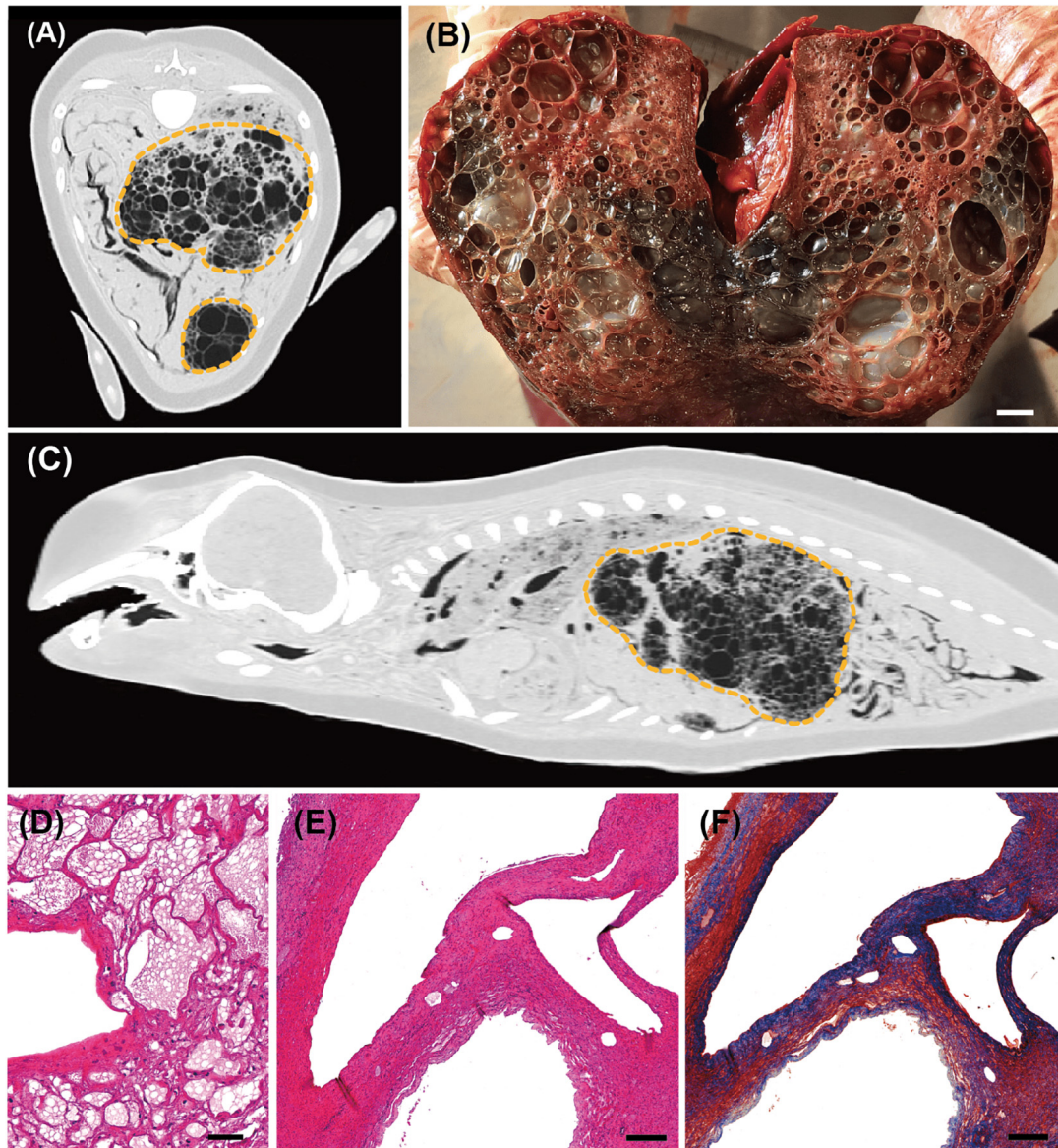


FIGURE 2 | Computed tomographic (CT), gross pathological, and histopathological findings in the liver of an East Asian finless porpoise (*Neophocaena asiaeorientalis sunameri*) carcass. **(A)** Transverse CT image (WL/WW: -500/1,400 HU) showing gas embolic lesions in the liver (yellow dotted lines). **(B)** Gross pathology of the liver parenchyma during necropsy. Scale bar = 1 cm. **(C)** Sagittal CT image (WL/WW: -500/1,400 HU) showing enlarged liver exerting pressure on both lungs and intestines. **(D)** Hematoxylin and eosin (H&E)-stained liver tissue showing both *in vivo* bubbles (<10 μm in diameter), and larger gas-filled cavities in sinusoids or veins. Scale bar = 40 μm . **(E)** Lower magnification of H&E-stained liver tissue showing larger bubbles. Scale bar = 200 μm . **(F)** Masson's trichrome-stained liver tissue of the same section as in **(E)**. Fibrotic tissues have been stained blue. Scale bar = 200 μm .

been reached. When the diver returns to the surface following a dramatic change in the diving pattern, gas solubility in the body system also decreases dramatically due to the reduction in ambient pressure. Once tissue gas become supersaturated as its partial pressure exceeds that of inhaled gas, *in vivo* bubbles may form that could result in gas embolism if they were to persist and enlarge, instead of being expelled.

There have been continuous reports of gas embolism in cetaceans in European, Mediterranean and American waters (Jepson et al., 2003; Fernández et al., 2005; Moore et al., 2009;

Siebert et al., 2013; Cuvertoret-Sanz et al., 2020; IJsseldijk et al., 2021). The present study is the first to report gas embolic lesions in a cetacean inhabiting Asian waters. Currently, it is postulated that gas embolic lesions in cetaceans may result from behavioral responses to anthropogenic causes such as naval sonar exercises, underwater detonation, and in-depth fishing that alter the animals' diving patterns (Jepson et al., 2003; Fernández et al., 2005; Moore et al., 2009; Danil and St. Leger, 2011; St. Leger et al., 2011). However, tagging studies to investigate the geographical range of East Asian finless porpoises is currently limited, making

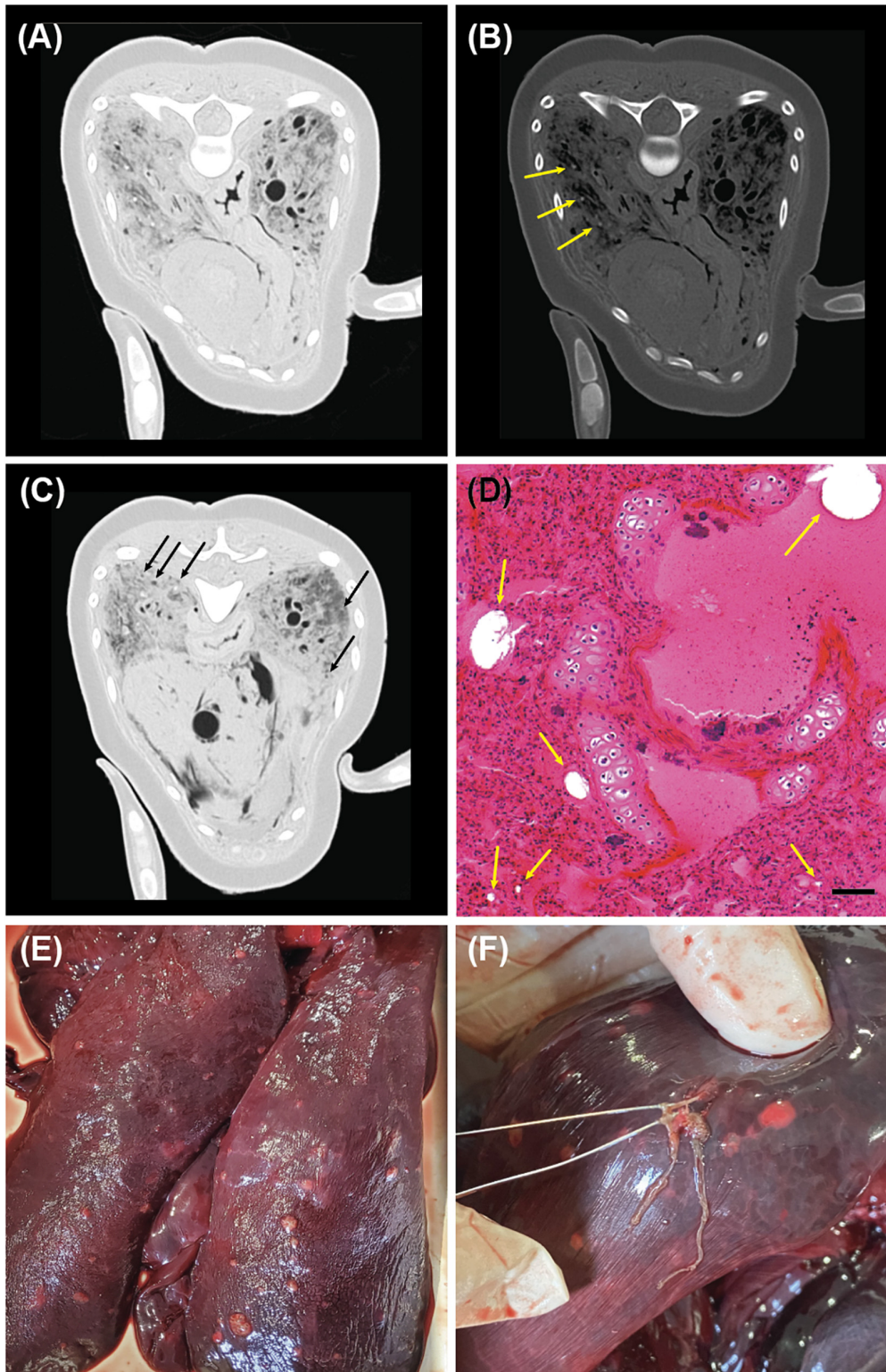


FIGURE 3 | Computed tomographic (CT), histopathological, and gross pathological findings in the lung of an East Asian finless porpoise (*Neophocaena asiaeorientalis sunameri*) carcass. **(A)** Transverse CT image (WL/WW: $-500/1,400$ HU) showing ground-glass opacities in the lungs. **(B)** Transverse CT image (WL/WW: $300/1,500$ HU) showing small hyper-attenuated fibrotic nodules (yellow arrows), which indicate parasitic pulmonary infection. **(C)** Transverse CT image (WL/WW: $-500/1,400$ HU) showing non-bronchiolar bubbles (black arrows) in both lung lobes. **(D)** Hematoxylin and eosin-stained lung tissue showing gas emboli (yellow arrows). Scale bar = $50\ \mu\text{m}$. **(E)** Surface feature of the lungs with nodules. **(F)** *Halocercus sunameri* found from the lung nodules.

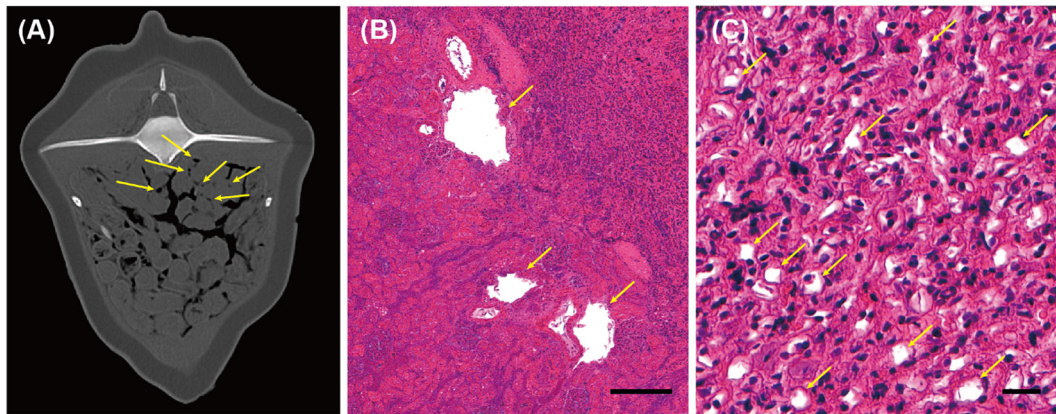


FIGURE 4 | Computed tomographic (CT) and histopathological findings in the kidney of an East Asian finless porpoise (*Neophocaena asiaeorientalis sunameri*) carcass. **(A)** Transverse CT image (WL/WW: 300/1,500 HU) of the kidney showing gas emboli (yellow arrows). Histopathology of hematoxylin and eosin -stained kidney tissue, showing **(B)** the boundary between the renal cortex and medulla, with gas-filled cavities (diameter $\leq 350 \mu\text{m}$) indicated by yellow arrows, and **(C)** *in vivo* bubbles (diameter $\leq 15 \mu\text{m}$), present among the cells (yellow arrows). Scale bar = $200 \mu\text{m}$ and $20 \mu\text{m}$ in **(B,C)**, respectively.

it impossible to backtrack the location of exposure that could have resulted in the event that rendered the animal susceptible to gas embolism. Therefore, conclusive evidence of the actual cause of death of the East Asian finless porpoise in the present study is unavailable.

In the present study, both lungs of the finless porpoise have exhibited heterogenous hyperattenuation pattern giving the appearance of pulmonary ground glass opacity on PMCT. The imaging pattern in this carcass is compatible with pneumonitis (Garg et al., 2019a,b; Hamel et al., 2020). Although the PMCT findings alone are not pathognomonic, the pulmonary ground glass opacity pattern in lungs is not likely caused by post-mortem changes due to absence of pulmonary hypostasis and post-mortem staining on body surface. In conjunction with the evidence of *Halocercus sunameri* infection in lung parenchyma, the finless porpoise is suspected to be suffering from decline of pulmonary function secondary to pneumonitis and parasitic infection.

Although the underlying reason between the cause of pneumonitis in lungs and gas embolic lesions cannot be concluded, we hypothesize that they can be mutual causative:

1. The East Asian finless porpoise had been unable to expel *in vivo* gas bubbles from its circulation as a result of decline of pulmonary function (Moon, 1996). (We suspected the latter to be secondary to parasitic or bacterial lung infection, but this could not be confirmed in the absence of bacterial swabs, which had not been collected prior to the carcass being frozen). Consequently, the gas bubbles agglomerated in the liver and enlarged while the animal might have experienced peracute underwater entrapment (Cuvertoret-Sanz et al., 2020) or was surfacing after diving, causing gas embolic lesions in the liver.
2. The East Asian finless porpoise had developed gas embolic lesions in the liver due to excessive tissue gas tension. The enlarged gas embolic lesions in the liver elevated the

diaphragms and caused atelectasis, which had resulted in pneumonitis and decreased pulmonary function (Russi, 1998).

Nonetheless, post-mortem investigations conducted herein also showed that body wasting, along with pneumonitis and *Halocercus sunameri* infection in lung parenchyma, might be related to the death of the animal (Wan et al., 2017).

To increase the diagnostic accuracy, reasonable death time estimation can facilitate the understanding of the degree of post-mortem change in carcass. One of the simplest ways is using the rectal temperature-based death time estimation, which provides useful information to infer the time since death of an animal. However, there is no previous research studying the death time estimation in wild cetaceans (Moore et al., 2020), not to mention the study on rectal temperature-based death time estimation in finless porpoise. To date, Cockcroft (1991) has reported the only reference for death time estimation in captive cetacean using one striped dolphin, which cannot be extrapolated to the finless porpoise of the present study due to the differences in size and shape of body mass.

Gas content analysis using gas chromatography has often been used for discrimination of putrefaction gases from gas embolism to verify decompression sickness (Pierucci and Gherson, 1968, 1969). Yet, accurate sampling of nitrogen and respiratory gases can be sometimes difficult (de Quirós et al., 2011). The application of PMCT prior to conventional necropsy can provide precise spatial information of the gas bubble lesions or gas embolism, in which it can facilitate proper necropsy planning and accurate gas sampling in the carcass during gas content analysis. However, due to lacking in the equipment required for gas sampling and gas content analysis in the laboratory, it is admittedly this process has not been done in the present study. We suggest future studies can confirm the gas content with gas chromatography in conjunction with PMCT. Conducting PMCT prior to conventional necropsy provided precise spatial

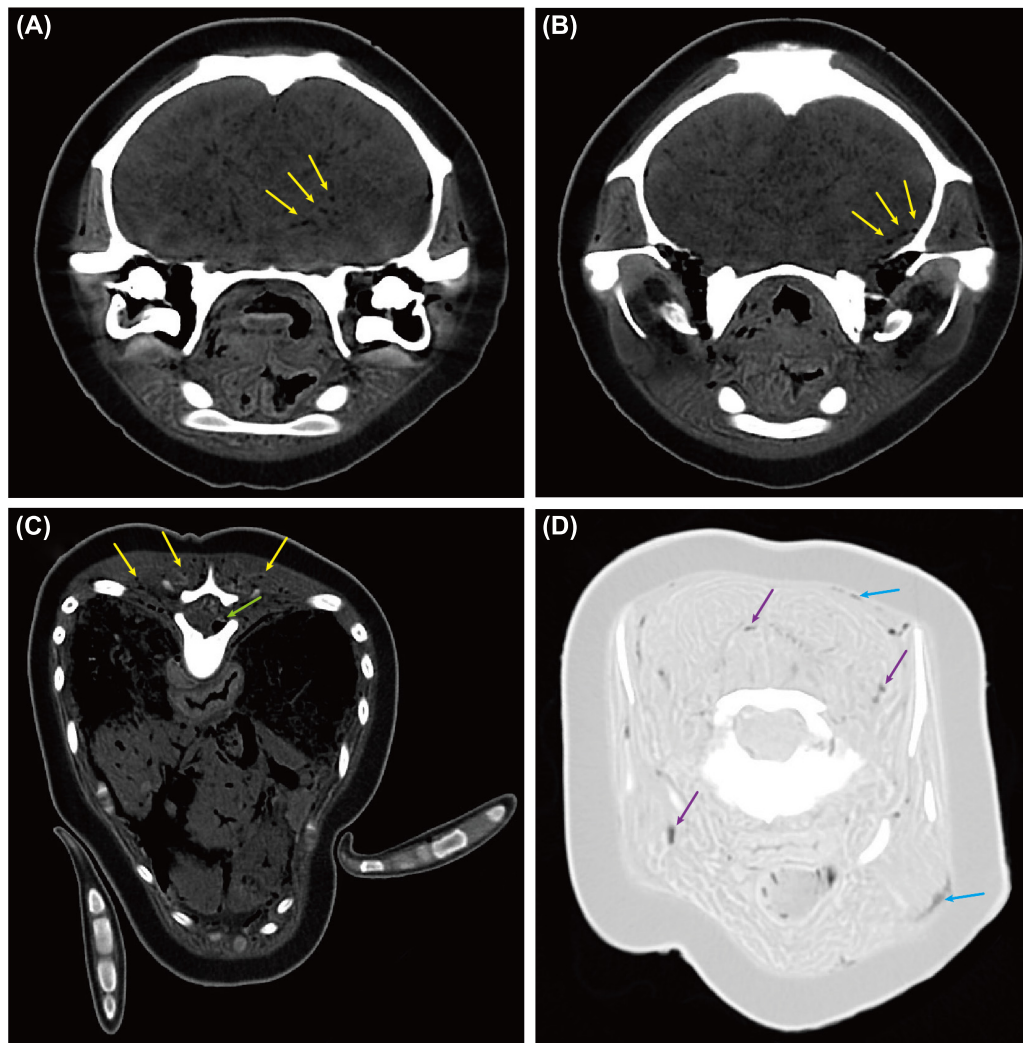


FIGURE 5 | Computed tomographic (CT) findings in the brain, spinal cord, muscles, and sub-dermal tissue of an East Asian finless porpoise (*Neophocaena asiaeorientalis sunameri*) carcass. Gas bubbles ranging from 0.7 to 3.0 mm in diameter were found through various tissues. **(A,B)** Transverse CT images (WL/WW: 152/524 HU) showing gas bubbles (yellow arrows) in brain tissue. **(C)** Transverse CT image (WL/WW: 152/524 HU) showing gas bubbles in epaxial muscles (yellow arrows) and spinal cord (green arrow). **(D)** Transverse CT image (WL/WW: -500/1,400 HU) showing gas bubbles in sub-dermal tissue (blue arrows) and cervical muscles (purple arrows).

information of gas bubble lesions or gas emboli, facilitating adequate necropsy planning. PMCT also provided superior diagnostic outcomes for identifying gas embolic lesions because of its high spatial resolution, contrast resolution, and signal-to-noise ratio. However, the diagnostic sensitivity of PMCT might be affected by the longitudinal partial volume effect, occurring when a CT slice containing a gas bubble (<0.5 mm in diameter) is partially occupied by body tissue—i.e., the gas bubble is smaller than the slice width. This degrades image resolution and contrast of the gas bubble in the CT image. Reducing the slice thickness should aid in limiting the impact of the partial volume effect. Moreover, histology of tissue samples should be conducted alongside PMCT, to confirm a gas embolism diagnosis. In the future, meta-analysis of death time estimation in cetaceans, in addition to rectal temperature-based method, is

crucial to facilitate the diagnostic accuracy during virtopsy and necropsy. It is also important to minimize the freeze artifact on the histopathology by performing necropsy without freezing the carcass. For this, more local base facilities for cetacean necropsy must be secured and a well-formed manpower network must be established in Korea.

CONCLUSION

This report is the first to identify gas embolism in an East Asian finless porpoise in Asian waters. Gas-filled cavitory lesions were identified throughout the stranded animal's body, especially in the liver, by PMCT. Most of the liver parenchyma was replaced by gas-filled cavitory lesions (0.5–25.0 mm in diameter),

making the organ virtually impossible to function normally. Liver cavities were surrounded by fibrotic capsules of 1.0–3.0 mm thickness, which contributed to physical pressure on surrounding organs by maintaining a firm and bubbly enlarged appearance of the liver. These lesions have been reported in previous studies as one of the representative aspects of gas embolism by decompression syndrome. As small-sized air bubbles that could have been missed in the necropsy were identified through PMCT, histological analysis was performed in organs other than the liver, and as a result, *in vivo* bubbles were identified in kidneys, lungs, mesenteric lymph node, and stomach wall. This case suggests that decompression syndrome can also occur in East Asian finless porpoise in Asian water, but as only limited information was obtained from frozen carcasses, investigation should be conducted with fresh carcass in the future to secure more detailed data.

DATA AVAILABILITY STATEMENT

The original contributions presented in the study are included in the article/supplementary material, further inquiries can be directed to the corresponding author/s.

ETHICS STATEMENT

Ethical review and approval were not required since no aspect of the animal's life was altered for the present study.

REFERENCES

- Blix, A. S., Walløe, L., and Messelt, E. B. (2013). On how whales avoid decompression sickness and why they sometimes strand. *J. Exp. Biol.* 216, 3385–3387. doi: 10.1242/jeb.087577
- Cheng, Z., Pine, M. K., Li, Y., Zuo, T., Niu, M., Wan, X., et al. (2021). Using local ecological knowledge to determine ecological status and threats of the East Asian finless porpoise. *Management* 203:105516.
- Chou, D. W., Jao, Y. T. F. N., and Han, S. C. (2016). Normal and abnormal gas patterns: which is which? *Intern. Emerg. Med.* 11, 147–148. doi: 10.1007/s11739-015-1266-9
- Cockcroft, V. G. (1991). Rate of post mortem temperature loss in a striped dolphin (*Stenella coeruleoalba*). *Aqu. Mamm.* 17, 88–90.
- Cuvertoret-Sanz, M., López-Figueroa, C., O'Byrne, A., Canturri, A., Martí-García, B., Pintado, E., et al. (2020). Causes of cetacean stranding and death on the Catalan coast (western Mediterranean Sea), 2012–2019. *Dis. Aquat. Organ.* 142, 239–253. doi: 10.3354/dao03550
- Danil, K., and St. Leger, J. A. (2011). Seabird and dolphin mortality associated with underwater detonation exercises. *Mar. Technol. Soc. J.* 45, 89–95
- Denk, M., Fahlman, A., Dennison-Gibby, S., Song, Z., and Moore, M. (2020). Hyperbaric tracheobronchial compression in cetaceans and pinnipeds. *J. Exp. Biol.* 223:jeb217885. doi: 10.1242/jeb.217885
- Danil, K., St. Leger, J. A., Dennison, S., de Quirós, Y. B., Scadeng, M., Nilson, E., et al. (2014). *Clostridium perfringens* septicemia in a long-beaked common dolphin *Delphinus capensis*: an etiology of gas bubble accumulation in cetaceans. *Dis. Aquat. Org.* 111, 183–90
- Dennison, S., Moore, M. J., Fahlman, A., Moore, K., Sharp, S., Harry, C. T., et al. (2012). Bubbles in live-stranded dolphins. *Proc. R. Soc. Lond.* 279, 1396–1404. doi: 10.1098/rspb.2011.1754

AUTHOR CONTRIBUTIONS

AY and SWK conceived the study, designed, prepared, and performed the necropsy, collected samples for analyses, analyzed the data, wrote the manuscript, and produced the figures. SBL prepared and set up the specimen for necropsy and sampling. SBL, YRL, SMK, JK, WJJ, and YML performed the necropsy. CP analyzed the data and produced the figures. SL and J-pS performed CTCP scanning and 3D rendering analysis. SMK performed parasite identification. SSG, SGK, and JWK prepared the necropsy, validated the data, and revised the manuscript. BYK collected the stranded carcass and supervised the necropsy on Jeju Island. SCP managed the application for funding and supervised the entire project. All authors contributed to the manuscript and approved the submitted version.

FUNDING

This research was supported by the Basic Research in Science and Engineering Program facilitated by the National Research Foundation (NRF) of Korea, and funded by the Ministry of Education (Grant No. 2018R1D1A1A02086128).

ACKNOWLEDGMENTS

We would like to thank Jeju National University Equine Hospital for providing access to their equipment for purposes of computed tomography.

- de Quirós, Y. B., González-Díaz, Ó., Saavedra, P., Arbelo, M., Sierra, E., Sacchini S., et al. (2011). Methodology for in situ gas sampling, transport and laboratory analysis of gases from stranded cetaceans. *Sci. Rep.* 1:193. doi: 10.1038/srep00193
- Elmegaard, S. L., Johnson, M., Madsen, P. T., and McDonald, B. I. (2016). Cognitive control of heart rate in diving harbor porpoises. *Curr. Biol.* 26, R1175–R1176. doi: 10.1016/j.cub.2016.10.020
- Fahlman, A., Moore, M. J., and Wells, R. S. (2021). How Do Marine Mammals Manage and Usually Avoid Gas Emboli Formation and Gas Embolic Pathology? Critical Clues From Studies of Wild Dolphins. *Front. Mar. Sci.* 8:598633. doi: 10.3389/fmars.2021.598633
- Fernández, A., Edwards, J. F., Rodriguez, F., De Los Monteros, A. E., Herraiz, P., Castro, P., et al. (2005). “Gas and fat embolic syndrome” involving a mass stranding of beaked whales (Family Ziphiidae) exposed to anthropogenic sonar signals. *Vet. Pathol.* 42, 446–457. doi: 10.1354/vp.42-4-446
- Fernández, A., Sierra, E., Díaz-Delgado, J., Sacchini, S., Sánchez-Paz, Y., Suárez-Santana, C., et al. (2017). Deadly acute Decompression Sickness in Risso's dolphins. *Sci. Rep.* 7:13621. doi: 10.1038/s41598-017-14038-z
- Geraci, J. R., and Lounsbury, V. J. (2005). *Marine Mammals Ashore: A field Guide for Strandings*. Baltimore: National Aquarium in Baltimore.
- Garg, M., Prabhakar, N., Gulati, A., Agarwal, R., and Dhooira, S. (2019a). Spectrum of imaging findings in pulmonary infections. Part 1: Bacterial and viral. *Pol. J. Radiol.* 84, e205–e213 doi: 10.5114/pjr.2019.85812
- Garg, M., Prabhakar, N., Gulati, A., Agarwal, R. and Dhooira, S. (2019b). Spectrum of imaging findings in pulmonary infections. Part 2: Fungal, mycobacterial, and parasitic. *Pol. J. Radiol.* 84, e214–e223 doi: 10.5114/pjr.2019.85813
- Hamel, P. E., Giglio, R. F., Cassle, S. E., Farina, L. L., Leone, A. M., and Walsh, M. T. (2020). Postmortem computed tomography and magnetic resonance imaging findings in a case of coinfection of dolphin morbillivirus and *aspergillus*

- fumigatus* in a juvenile bottlenose dolphin (*Tursiops truncatus*). *J. Zoo Wildl. Med.* 51, 448–454 doi: 10.1638/2019-0087
- Ijsseldijk, L. L., Scheidat, M., Siemensma, M. L., Couperus, B., Leopold, M. F., Morell, M., et al. (2021). Challenges in the Assessment of Bycatch: Postmortem Findings in Harbor Porpoises (*Phocoena phocoena*) Retrieved From Gillnets. *Vet. Pathol.* 58, 405–415. doi: 10.1177/0300985820972454
- Jefferson, T. A., and Hung, S. K. (2004). *Neophocaena phocaenoides*. *Mamm. Species.* 746, 1–12. doi: 10.1644/746
- Jepson, P. D., Arbelo, M., Deaville, R., Patterson, I. A. P., Castro, P., Baker, J. R., et al. (2003). Gas-bubble lesions in stranded cetaceans. *Nature* 425, 575–576.
- Jepson, P. D., Deaville, R., Patterson, I. A. P., Pocknell, A. M., Ross, H. M., Baker, J. R., et al. (2005). Acute and Chronic Gas Bubble Lesions in Cetaceans Stranded in the United Kingdom. *Vet. Pathol.* 42, 291–305. doi: 10.1354/vp.42-3-291
- Kooyman, G. L., Schroeder, J. P., Denison, D. M., Hammond, D. D., Wright, J. J., and Bergman, W. P. (1972). Blood nitrogen tensions of seals during simulated deep dives. *Am. J. Physiol.* 223, 1016–1102. doi: 10.1152/ajplegacy.1972.223.5.1016
- Kot, B. C. W., Tsui, H. C. L., Chung, T. Y. T., and Lau, A. P. Y. (2020). Postmortem neuroimaging of cetacean brains using computed tomography and magnetic resonance imaging. *Front. Mar. Sci.* 7:544037. doi: 10.3389/fmars.2020.544037
- Laurent, P. E., Coulange, M., Mancini, J., Bartoli, C., Desfeux, J., Piercecchi-Marti, M. D., et al. (2014). Postmortem CT appearance of gas collections in fatal diving accidents. *AJR Am. J. Roentgenol.* 203, 468–475 doi: 10.2214/AJR.13.12063
- Moon, R. E. (1996). “Gas embolism,” in *Handbook on hyperbaric medicine*, eds. G. Oriani, A. Marroni, and F. Wattel (Springer: Berlin Heidelberg New York), 229–248
- Moore, M. J., Mitchell, G. H., Rowles, T. K., Early, G. (2020). Dead Cetacean? Beach, Bloat, Float, Sink. *Front. Marine Sci.* 7:333. doi: 10.3389/fmars.2020.00333
- Moore, M. J., Bogomolni, A. L., Dennison, S. E., Early, G., Garner, M. M., Hayward, B. A., et al. (2009). Gas bubbles in seals, dolphins, and porpoises entangled and drowned at depth in gillnets. *Vet. Pathol.* 46, 536–547. doi: 10.1354/vp.08-VP-0065-M-FL
- Pierucci, G. and Gherson, G. (1968). Experimental study on gas embolism with special reference to the differentiation between embolic gas and putrefaction gas. *Zacchia* 4, 347–73
- Pierucci, G. and Gherson, G. (1969). Further contribution to the chemical diagnosis of gas embolism. The demonstration of hydrogen as an expression of “putrefactive component”. *Zacchia* 5, 595–603
- Plattner, T., Thali, M. J., Yen, K., Sonnenschein, M., Stoupis, C., Vock, P., et al. (2003). Virtopsy-postmortem multislice computed tomography (MSCT) and magnetic resonance imaging (MRI) in a fatal scuba diving incident. *J. Forensic Sci.* 48, 1347–1355.
- Pugliares, K. R., Bogomolni, A., Touhey, K. M., Herzig, S. M., Harry, C. T., and Moore, M. J. (2007). Marine mammal necropsy: an introductory guide for stranding responders and field biologists. *Woods Hole Ocean. Instit. Tech. Doc.* 6:117.
- Ridgway, S. H., and Howard, R. (1979). Dolphin lung collapse and intramuscular circulation during free diving: evidence from nitrogen washout. *Science* 206 1182–1183. doi: 10.1126/science.505001
- Russi, E. W. (1998). Diving and the risk of barotrauma. *Thorax* 53, S20–S24.
- Schwartz, T., Gough-Fibkins, S., Santini, R., and Kopylov, D. (2018). Abdominal CT Scan Findings of Decompression Sickness: A Case Report. *J. Radiol. Case Rep.* 12, 17–23.
- Shedge, R., Krishan, K., Warriar, V., and Kanchan, T. (2021). *Postmortem changes*. Florida: StatPearls Publishing.
- Siebert, U., Jepson, P. D., and Wohlsein, P. (2013). First indication of gas embolism in a harbour porpoise (*Phocoena phocoena*) from German waters. *Eur. J. Wildl. Res.* 59, 441–444.
- Southall, B. L., Nowacek, D. P., Miller, P. J., and Tyack, P. L. (2016). Experimental field studies to measure behavioral responses of cetaceans to sonar. *Endanger. Species Res.* 31, 293–315.
- St. Leger, J. A., Danil, K., Dennison, S., Scadeng, M., de Quirós, Y. B. M., Fernandez, T., et al. (2011). “Pathology of barotrauma in long-beaked common dolphins (*Delphinus capensis*),” in *Proceedings of the 19th Biennial Conference on the Biology of Marine Mammals*, (Tampa, Florida).
- Wan, X. L., Zheng, J. S., Li, W. X., Zeng, X. Y., Yang, J. W., Hao, Y. J., et al. (2017). Parasitic infections in the East Asian finless porpoise *Neophocaena asiaeorientalis sunameri* living off the Chinese Yellow/Bohai Sea coast. *Dis. Aquat. Organ.* 125, 63–71. doi: 10.3354/dao03131
- Xiong, X., Chen, X., Zhang, K., Mei, Z., Hao, Y., Zheng, J., et al. (2018). Microplastics in the intestinal tracts of East Asian finless porpoises (*Neophocaena asiaeorientalis sunameri*) from Yellow Sea and Bohai Sea of China. *Mar. Pollut. Bull.* 136, 55–60. doi: 10.1016/j.marpolbul.2018.09.006
- Yamaguti, S. (1951). Studies on the helminth fauna of Japan. Part 46. Nematodes of Marine Mammals. With 3 Plates. *Arbeiten aus der Medizinischen Fakultät Okayama* 7, 295–306.
- Yuen, A. H. L., Tsui, H. C. L., and Kot, B. C. W. (2016). “Preliminary Assessment of Cranial Cervical Dislocation in Stranded Cetaceans Using Multislice Computed Tomography,” in *Proceedings of the 47th International Association for Aquatic Animal Medicine*, (Virginia Beach, VA).
- Yuen, A. H. L., Tsui, H. C. L., and Kot, B. C. W. (2017). Accuracy and reliability of cetacean cranial measurements using computed tomography three dimensional volume rendered images. *PLoS One* 12:e0174215. doi: 10.1371/journal.pone.0174215
- Zeng, X., Ji, J., Hao, Y., and Wang, D. (2015). Topographical distribution of blubber in finless porpoises (*Neophocaena asiaeorientalis sunameri*): a result from adapting to living in coastal waters. *Zool. Stud.* 54:e32. doi: 10.1186/s40555-015-0111-1

Conflict of Interest: The authors declare that the research was conducted in the absence of any commercial or financial relationships that could be construed as a potential conflict of interest.

Publisher’s Note: All claims expressed in this article are solely those of the authors and do not necessarily represent those of their affiliated organizations, or those of the publisher, the editors and the reviewers. Any product that may be evaluated in this article, or claim that may be made by its manufacturer, is not guaranteed or endorsed by the publisher.

Copyright © 2022 Yuen, Kim, Lee, Lee, Lee, Kim, Poon, Kwon, Jung, Giri, Kim, Kang, Lee, Seo, Kim and Park. This is an open-access article distributed under the terms of the Creative Commons Attribution License (CC BY). The use, distribution or reproduction in other forums is permitted, provided the original author(s) and the copyright owner(s) are credited and that the original publication in this journal is cited, in accordance with accepted academic practice. No use, distribution or reproduction is permitted which does not comply with these terms.